Quantified Symmetry for Entorhinal Spatial Maps

Erick Chastain*, Yanxi Liu†

February 6, 2006

Abstract

General navigation requires a spatial map that is not anchored to one environment. The firing fields of the "grid cells" found in the rat dorsolateral medial entorhinal cortex (dMEC) could be such a map. Our work provides an explanation for how the context-independent properties of "grid cell" firing arise. We use computational means to analyze and validate the geometric and algebraic invariant properties of the firing fields, leading to a context-independent spatial map. Our method computes the specific symmetry group implicitly associated with the spatial map, and quantifies the regularity of the firing fields to achieve a symmetry-based clustering into two different types of "grid cells." This quantified regularity makes spatial mapping more computationally efficient and suggests a way to use the dMEC firing patterns to decode the rat's position in the room. Finally, the highly invariant lattice structure of a "grid cell" firing field encodes the rat's position with sufficient redundancy to remain the same under changes in the shape of the room. Thus we show formally how the context-independent properties of "grid cells" can arise from their invariance under transformation.

1 Introduction

Place cell representation is context[20][14] and task-specific[11], while general navigation requires a more abstract map that is not anchored to one environment. It has been hypothesized that there exists a representation upstream of the rat hippocampus that is context-independent [17] [16] [19]. This general spatial map is just a component of a distributed network [16] which is the basis for navigation [21] [13]. One potential possibility for such a map is the multi-peaked firing field found in dorsolateral medial entorhinal cortex (dMEC), which accurately represent the rat's position [3] in a near-regular grid [5]. This is in sharp contrast to place cells' one-peak firing fields [13] [12]. Using symmetry analysis and information theory, we provide a justification for the hypothesis that dMEC grid cells can be the basis for a general spatial map (see also Chastain & Liu 2006 [2]). We show that the geometric and algebraic invariant properties of the firing fields imply the context-independence of the dMEC spatial map.

*E-mail: echastai@cnbc.cmu.edu, Dept. of Computer Science, Carnegie Mellon University, USA

†E-mail: yanxi@cs.cmu.edu, The Robotics Institute, Carnegie Mellon University, USA

2 Context-Independence and The Structure of Grid Cells

Hafting et al.'s data on grid cells suggests that dMEC firing fields are near-regular [5]. Accordingly, we applied Liu et al.'s [8] algorithm on Hafting et al.'s [5] data (from the 2m diameter circular enclosure) to find the nearest regular lattice [9] of each grid cell's firing field. The algorithm takes a user-specified lattice D_L and finds the nearest regular lattice by minimizing the following energy functional:

$$E_R = \sum_{i=1}^{N_i}(l_i - ||T_1||)^2 + \sum_{j=1}^{N_j}(l_j - ||T_2||)^2 + \sum_{k=1}^{N_k}(l_k - ||T_1 + T_2||)^2 + \sum_{m=1}^{N_m}(l_m - ||T_1 - T_2||)^2$$

where l_i, l_j, l_k, and l_m are the lengths of the links in the lattice D_L corresponding to links in the regular lattice R_L along the directions of T_1, T_2, $T_1 + T_2$, and $T_1 - T_2$, respectively. N_i, N_j, N_k , N_m are the total number of links in D_L, and θ is the angle between T_1 and T_2 [8]. Vectors T_1 and T_2 form the boundary of a generating tile and can be used to generate the entire lattice (Figure 1).The results of using this analysis on the firing fields are illustrated in Figure 1. To the left (in Figure 1) is the original lattice, fitted by hand using the same user interface that was used by Liu et al. [8]. To the right (in Figure 1) is the regularized lattice, with image pixels morphed accordingly. The figure shows three of the eleven firing field lattices fitted using this algorithm.

2.1 Regularity Quantification of Grid Cells

In addition, we used two regularity measures proposed by Liu et al. [8], the **G** score (geometric regularity) and the **A** score (firing rate regularity). The **G** score is proportional to the change in energy E_R needed to regularize the lattice (with higher scores corresponding to higher irregularity). The **A** score is the average standard deviation of all corresponding pixels in all lattice tiles (with a gaussian noise model). Textures with a regular pattern have $G = 0$ and $A = 0$. Type I near-regular

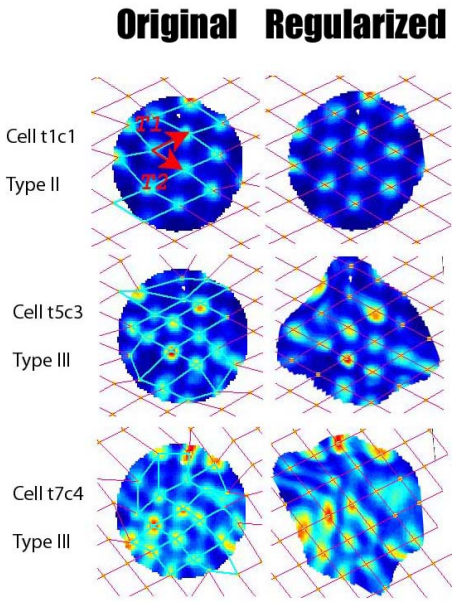

Figure 1: These are the firing field lattices of three different grid cells. The generating vectors T_1 and T_2 are indicated in red.

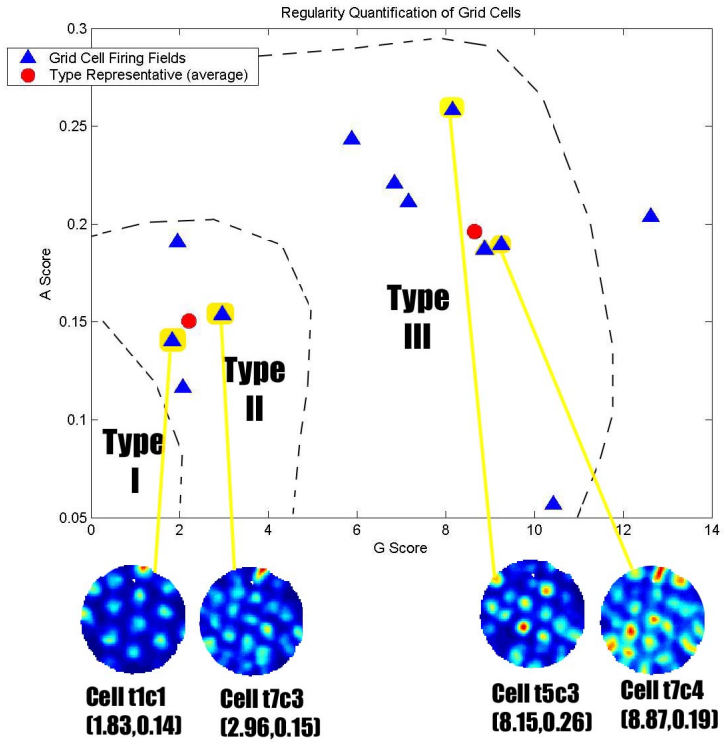

Figure 2: A plot of the **G** and **A** scores of all 11 grid cells fitted with regularized lattices. Clustering was done using k-means. The first (leftmost) cluster of grid cells falls within type II Near-regular Lattices, and the second cluster of grid cells is of Type III, according to Liu's classification of Near-regular Lattices and Textures. [8]

textures (NRTs) have **G** close to zero and $A > 0$. Type II NRTs have $G > 0$ and **A** closer to zero. Type III (irregular) NRTs have **G** and **A** scores much further from zero [8].

If we compute the **G** and **A** scores for all eleven of the grid cell lattice tiles, they form two clusters (see Figure 2). In Liu's classification of near-regular textures, the two clusters fall squarely within type II and III NRT's. Firing field lattices of type II are significantly more geometrically regular than that of the type III, but both have the same hexagonal lattice topology. Because of the demonstrated high regularity of each firing field, redundancy in encoding the rat's position is also high [10]. Thus in order to have sufficient information to decode the rat's position, it is necessary to use multiple grid cells. Grid cells show variability between cell firing fields in both orientation and inter-peak spacing [5]. Because the regularity of the spacing has two clusters, we can take the centroid of each to represent each type of variability in spacing.To account for the variability of orientation between grids, these representatives are rotated by different degrees and integrated temporally (the most robust method involving finding the posterior distribution of the position given the cell responses [15]). We hypothesize that grid cells can represent the rat's position by integrating the firings of just a few cells due to the limited variability in spacing (as there are only two clusters for inter-peak spacing in Figure 2).

This observation was verified using bayesian decoding by Fyhn et al. [3] and is stated explicitly as a hypothesis by Hafting et al. [5]. Fyhn et al.'s estimate of the minimum number of grid cells required to decode the rat's position is eight [3], which is a feasible prediction of our model if we simplify orientation by exploiting rotational invariance. The number of cells whose activity must be integrated to decode position is exponential in the number of distinct inter-peak distances. The number of cells required to decode position is of this form because we must integrate all possible variations in orientation for each distinct inter-peak spacing. Therefore a low number of distinct inter-peak spacings is essential to efficiently decode position.

2.2 Invariance properties of Grid Cell Firing Fields

The firing fields of grid cells are invariant under many different transformations, as can be seen in Figure 3. The type of regularized lattice fit to the firing fields, which has symmetry group *p6m*, has in fact been proven to be a maximally redundant packing of the plane [22] [7]. Due to this high redundancy, the grid cell encoding of position has many equivalent responses under transformations of position. A change in the geometry of the room can be thought of as changing the possible positions in the room that the rat can visit. The possible positions for the rat to visit in the new room are transformed versions of positions possible for the rat to visit in the old room. Because there are so few distinct grid cell responses under transformations of position it is evident that grid cell responses encode position in a way that is robust to changes in room geometry. Hafting et al. have observed this context independence as well [6]. This suggests that the invariant properties of grid cell firing fields make the dMEC spatial map highly context-independent. The symmetry-based analysis we used identifies one of the 17 wallpaper groups [1], p6m, as the symmetry group of the deformed firing field of dMEC. Near-regularity analysis provides a computable quantitative measurement for the different types of lattice tiles in the firing field. Algebraically and geometrically, the group theoretical approach leads us to a deeper computational understanding of the context-independent properties of the dMEC spatial map.

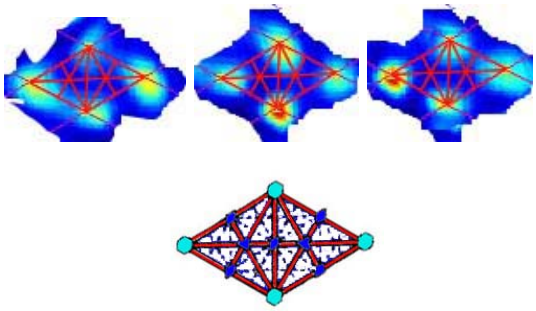

Figure 3: These are the first, fourth, and seventh tiles of cell t5c3 and the *p6m* symmetry group tile which we fit onto grid cell firing fields. We can model the approximate invariance properties by computing the symmetry group of the lattice form, since the firing field regularity is sufficiently high. The three tiles from t5c3 are highly bilaterally symmetric, as can be seen by the similarity of both sides with respect to the axes demarcated by the red lines. A *p6m* tile has outer vertices that are invariant under 60 degree rotation, and is bilaterally symmetric along all of the solid lines. Diamonds signify invariance under 180 degree rotation around that point, and triangles signify invariance under 120 degree rotation around that point. All tiles have invariance under translations that are multiples of their generating vectors T_1 and T_2.

References

[1] Coxeter, H.S.M. and Moser, W.O.J. Generators and Relations for Discrete Groups, 4th edn. (Springer-Verlag, New York, 1980).

[2] Chastain, E., and Liu, Y. Firing Fields of Dorsocaudal Medial Entorhinal Cortex as a Context-Independent Spatial Map. Robotics Institute Tech Report, Number 06-02 (2006).

[3] Fyhn, M., Molden, S., Witter, M. P., Moser, E. I. & Moser, M. B. Spatial representation in the entorhinal cortex. Science 305, 1258-1264 (2004).

[4] Grunbaum, B. and Shephard, G.C. Tilings and Patterns, (W.H. Freeman and Company, New York, 1987).

[5] Hafting, T., Fyhn, M., Molden, S., Moser, M., & Moser, E. I. Microstructure of a spatial map in the entorhinal cortex. Nature 436, 801-806 (2005).

[6] Hafting, T., By Communication (2005).

[7] Kuperberg, G. Notions of denseness. Geometry & Topology 4, 277-292, (2000).

[8] Liu, Y., Lin, W. C. & Hays, J. Near-Regular Texture Analysis and Manipulation, SIGGRAPH 2004.

[9] Liu, Y., Tsin, Y., & Lin, W. C. The Promise and Perils of Near-Regular Texture, International Journal of Computer Vision, 62, No. 1-2, 145-159, (2005).

[10] MacKay, D., Information Theory, Inference, & Learning Algorithms. (Cambridge University Press, 2002)

[11] Markus, E.J., Qin, Y., Leonard, B., Skaggs, W.E., McNaughton, B.L., Acknowledgments and Barnes, C.A. Interactions between location and task affect the spatial and directional firing of hippocampal neurons. J. Neurosci. 15, 7079-7094, (1995).

[12] OKeefe, J. & Nadel, L. The hippocampus as a Cognitive Map (Clarendon, Oxford, 1978).

[13] OKeefe, J. & Conway, D. H. Hippocampal place units in the freely moving rat: why they fire where they fire. Exp. Brain Res. 31, 573-590 (1978).

[14] OKeefe, J. & Burgess, N. Geometric determinants of the place fields of hippocampal neurons. Nature 381, 425-428 (1996).

[15] Pouget, A., Dayan, P., Zemel, R. Inference and Computation with Population Codes. Annual Review Neuroscience, 26, 381-410 (2003).

[16] Redish, A. D. Beyond the Cognitive Map: From Place Cells to Episodic Memory (MIT Press, Cambridge, 1999).

[17] Redish, A. D. & Touretzky, D. S. Cognitive maps beyond the hippocampus. Hippocampus 7, 15-35 (1997).

[18] Schattschneider, D., The Plane Symmetry Groups: Their Recognition and Notation, Am. Math. Monthly, 85, 439-450 (1978).

[19] Sharp, P. E. Complimentary roles for hippocampal versus subicular/entorhinal place cells in coding place, context, and events. Hippocampus 9, 432-443 (1999).

[20] Squire, L. R., Stark, C. E. & Clark, R. E. The medial temporal lobe. Annu. Rev. Neurosci. 27, 279-306 (2004).

[21] Taube, J. S. Head direction cells and the neurophysiological basis for a sense of direction. Prog. Neurobiol. 55, 225-256 (1998).

[22] Toth, L. F. Lagerungen in der Ebene, auf der Kugel und in Raum. (Springer-Verlag, Berlin, 1972).